

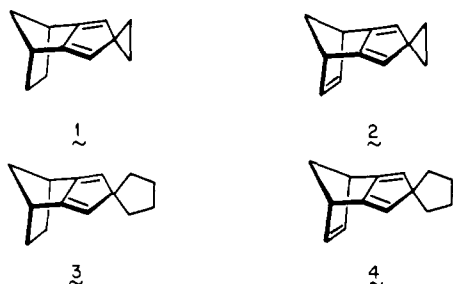
Stereoselectivity of Diels–Alder Cycloadditions to Norbornyl- and Norbornenyl-Fused Spirocyclic Cyclopentadiene Systems¹

Leo A. Paquette,^{*2a} Pana Charumilind,^{2a} Michael C. Böhm,^{2b} Rolf Gleiter,^{*2b} Lawrence S. Bass,^{2c} and Jon Clardy^{2c}

Contribution from the Evans Chemical Laboratories, The Ohio State University, Columbus, Ohio 43210, Institut für Organische Chemie der Universität Heidelberg, D-6900 Heidelberg, West Germany, and Department of Chemistry–Baker Laboratory, Cornell University, Ithaca, New York 14853. Received July 15, 1982

Abstract: The question of long-range stereoelectronic control in Diels–Alder reactions was studied by examining the stereoselectivity of dienophile addition to the four spirocyclic dienes **1–4**. The two spirocyclopropane derivatives (**1** and **2**) exhibit a strong predilection for below-plane attack with a wide range of dienophiles to give adducts having *syn*-sesquinorbornene geometry. In contrast, spirocyclopentane **3** enters into [4 + 2] cycloaddition totally by top-face bonding to generate *anti*-sesquinorbornene derivatives, except when dimethyl acetylenedicarboxylate is involved. The added double bond in **4** induces a loss in stereoselectivity. The PE spectra of **1** and **3** have been recorded and the ground-state electronic character of these dienes has been analyzed by detailed computational methods. The range of factors which are potentially able to account for these stereochemical phenomena is discussed. The best rationalization to this time deals with σ orbital mixing with the π_2 diene orbital, such interactions serving to tilt the diene orbitals with resultant minimization of antibonding influences on the bottom surface of **1** and top face of **3**.

This report deals with the stereochemical features of Diels–Alder reactions to four spirocyclopentadienes (**1–4**) in which the



unsaturated five-membered rings are fused to norbornyl and norbornenyl moieties. These substrates, made available through spiroalkylation of the corresponding cyclopentadienide anions,¹ are representative of 5,5-dialkylated cyclopentadienes which differ appreciably in the extent of electronic interaction imparted from the σ electrons of the saturated spirocyclic ring to the cyclopentadiene π network. Thus, the ground-state structures of **3** and **4** should be substantially the same as those of the corresponding gem-dimethyl derivatives. In contrast, the electronic features of cyclopropyl congeners **1** and **2** can be expected to differ significantly.^{3–5} When the long-range interactions of the norbornyl and norbornenyl fragments are superimposed upon these networks, the two faces of each of the diene rings become nonequivalent and differentiable.^{6a} At issue is to what degree and in what direction this π -facial stereoselectivity will be demonstrated. To enable proper comparisons to be made, the stereoselection exhibited by

Table I. Selected ¹³C Chemical Shifts in the Cycloadducts Derived from **1** (ppm, CDCl₃ Solution)^a

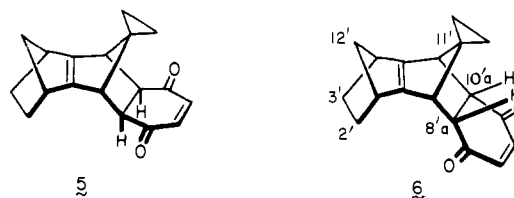
compd	C ₂ ', C ₃ '	C ₁₂ '	C ₁₁ '	C ₈ ' _a , C ₁₀ ' _a
5	25.49	50.19	44.24	55.16
6	25.79	50.43	52.31	52.80
7	25.05	50.15	44.08	66.46
	26.07			30.15
8	26.22	46.75	53.65	66.22
	26.51			31.36
9	25.88 ^b	49.91	45.44	25.59 ^b
13	25.29	50.01	41.56	52.00
14	25.73	50.25	57.05	49.76
16	22.58	48.01	66.22	150.06

^a See formula 6 for numbering scheme. ^b These values are possibly interchanged.

the gem-dimethyl analogues is reported in the ensuing paper.^{6b}

Results

4',5',6',7'-Tetrahydrospiro[cyclopropane-1,2'-(4,7)methano-[2H]indene (**1**). Although four isomeric adducts can arise from the Diels–Alder addition of **1** to *p*-benzoquinone, two products were obtained in a 62:38 ratio when reaction was conducted in chloroform solution at room temperature. In the ¹H NMR spectrum of the major component, the negligible coupling constant between the tetrahedral α -carbonyl and bridgehead protons (singlets at δ 2.97 and 2.50) implicated an *exo* orientation for the dienophile moiety.⁷ However, the spectral data did not permit a distinction between above-plane or below-plane attack. This question was resolved by X-ray crystal structure analysis which unambiguously demonstrated the principal adduct to be **5** (Figure 1). The *endo* nature of adduct **6** was ascertained by means of



a 3-Hz vicinal coupling operating on the saturated α -carbonyl

(7) See, for example: Marchand, A. P.; Rose, J. E. *J. Am. Chem. Soc.* **1968**, *90*, 3724.

(1) Electronic Control of Stereoselectivity. 15. For part 14, see: Paquette, L. A.; Charumilind, P.; Kravetz, T. M.; Böhm, M. C.; Gleiter, R. *J. Am. Chem. Soc.* **1983**, *105* (first paper of this series in this issue).

(2) (a) Columbus. (b) Heidelberg. (c) Ithaca; author to whom questions regarding the X-ray analyses should be directed.

(3) Gleiter, R.; Heilbronner, E.; de Meijere, A. *Helv. Chim. Acta* **1971**, *54*, 1029.

(4) Bischof, P.; Gleiter, R.; Heilbronner, E.; Hornung, V.; Schröder, G. *Helv. Chim. Acta* **1970**, *53*, 1645.

(5) Gleiter, R. *Top. Curr. Chem.* **1979**, *86*, 197 and references cited therein.

(6) (a) Paquette, L. A.; Charumilind, P. *J. Am. Chem. Soc.* **1982**, *104*, 3749. (b) Paquette, L. A.; Hayes, P. C.; Charumilind, P.; Böhm, M. C.; Gleiter, R.; Blount, J. F. *Ibid.* **1983**, *105* (third paper of this series in this issue).

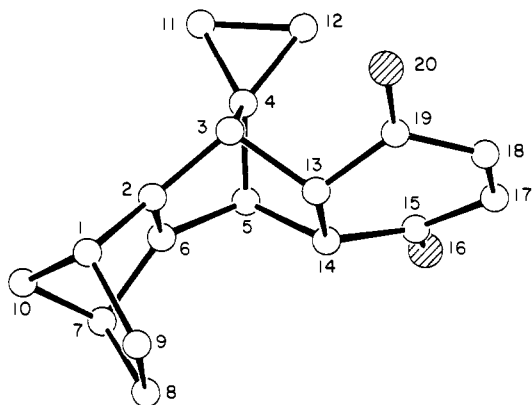


Figure 1. A computer-generated perspective drawing of the final X-ray model of **5** (hydrogens are omitted for clarity).

methine centers. When compared to that of **5**, the ^{13}C NMR spectrum of **6** shows that C2', C3', and C12' are not affected by the change in orientation of the oxygenated ring (Table I). Whereas similar phenomena are encountered in other adduct pairs which share *syn*-sesquinorbornene frameworks, a noticeable shift in the C12' signal generally accompanies crossover to the anti series (see below). On this basis, **6** was assigned the *syn* stereochemistry so that **1** is seen to react with benzoquinone strictly with below-plane stereoselectivity.⁸ The lack of adherence to the Alder rule is the obvious result of nonbonded interactions with C2' and C3' in the two relevant transition states and is of no real theoretical consequence.

In our examination of the reaction between the weakly dienophilic phenyl vinyl sulfone reagent and **1**, a pair of adducts (60:40 ratio) was again formed after 6 days in refluxing toluene. The major component of this readily separated mixture was shown to be **7** by X-ray analysis (Figure 2). The endo orientation of

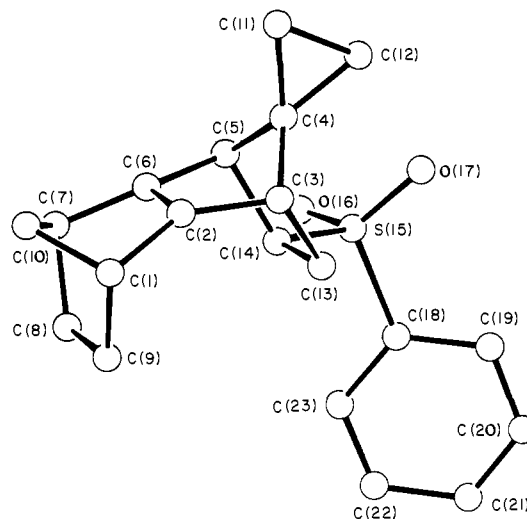
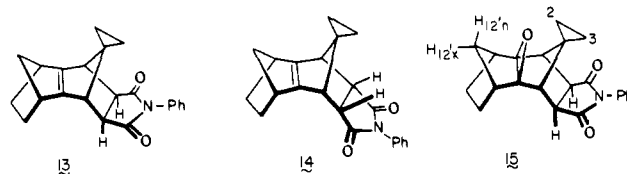


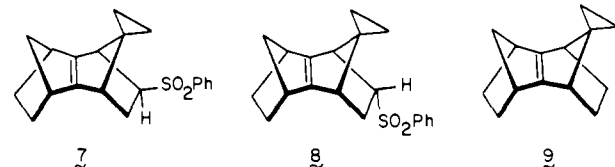
Figure 2. A computer-generated perspective drawing of the final X-ray model of **7** (hydrogens are omitted for clarity).

Similarly, *N*-phenylmaleimide added to **1** at room temperature with high below-plane stereoselectivity to give **13** and **14** in a 77:23

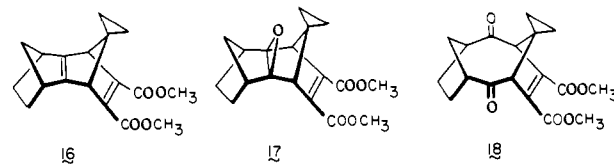
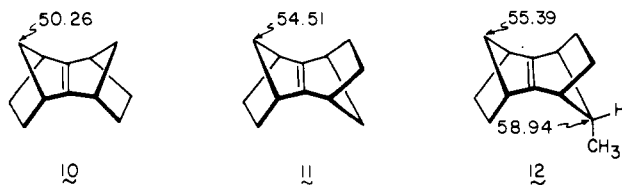


ratio. When **14** was stirred at room temperature in benzene solution for 12 days or heated at 50 °C in CDCl_3 for 3 days, no trace of the other three possible isomeric adducts could be detected, thus suggesting that the cycloaddition process is kinetically controlled (if thermodynamically controlled, the more stable **13** should have been produced). The structural assignments to **13** and **14** follow from their ^1H and ^{13}C NMR spectra (Table I). Additionally, **13** was slowly converted to **15** in the presence of *m*-chloroperbenzoic acid as expected of *syn*-sesquinorbornene derivatives.^{12a} In this derivative, the magnetic anisotropy of the oxirane ring^{12b} causes H12'_n to experience dramatic downfield shifting (to δ 2.15) relative to H12'_x (δ 1.55). Expectedly, the influence of the epoxide oxygen on the nearby cyclopropane ring is lessened; however, the exo methylene pair (δ 0.63) is notably deshielded relative to its endo counterpart (δ 0.43).

When **1** was admixed with the more reactive dimethyl acetylenedicarboxylate (DMAD) in chloroform solution at room temperature, cycloaddition proceeded rapidly to completion within 4 h and the lone adduct **16** was produced. That dienophile ste-



the phenylsulfonamide group in **8** follows as before from its ^1H NMR spectrum. The *syn* configuration of its methano bridges was deduced from the ^{13}C NMR spectrum. In particular, the close similarity of its C12' signal to that exhibited by **7** and **9** (made available for reference purposes by sodium amalgam reduction⁹ of **7**) is particularly diagnostic (Table I). The parallelism between these compounds and parent hydrocarbon **10**¹⁰ is quite evident. The contrasting downfield positions of the methano bridge carbons in **11**¹¹ and **12**⁶ require no additional comment.



reoselection had again occurred below plane in this instance was revealed by the ^{13}C NMR spectrum (Table I) and the high propensity exhibited by **16** for oxidation.¹¹ When simply allowed to stand in air, conversion to a mixture of **17** and **18** was noted. In contrast, peracid oxidation led exclusively to **17**. The differing facets of these reactions have been previously discussed.¹¹ The *syn* orientation of the methano bridges in **16** and **17** is made particularly apparent upon inspection of their ^1H NMR spectra (Figure 3). The widely different chemical shifts of H12'_n and

(8) In all of the examples reported herein, ^1H and ^{13}C NMR spectra were recorded prior to any purification, as well as on the isolated adducts. Also, TLC analyses were carried out directly on the unpurified reaction mixtures and subsequent to separation of the components. In no instance were other isomers observed; viz., the spectra and TLC plates could be duplicated by admixing of the isolated adducts in the proper amounts.

(9) Trost, B. M.; Arndt, H. C.; Stregge, P. E.; Verhoeven, T. R. *Tetrahedron Lett.* **1976**, 3477.

(10) (a) Paquette, L. A.; Carr, R. V. C.; Böhm, M. C.; Gleiter, R. *J. Am. Chem. Soc.* **1980**, *102*, 1186. (b) Böhm, M. C.; Carr, R. V. C.; Gleiter, R.; Paquette, L. A. *Ibid.* **1980**, *102*, 7218.

(11) Bartlett, P. D.; Blakeney, A. J.; Kimura, M.; Watson, W. H. *J. Am. Chem. Soc.* **1980**, *102*, 1383.

(12) (a) Paquette, L. A.; Carr, R. V. C. *J. Am. Chem. Soc.* **1980**, *102*, 7553. (b) Paquette, L. A.; Kravetz, T. M.; Böhm, M. C.; Gleiter, R. *J. Org. Chem.* **1983**, *48*,

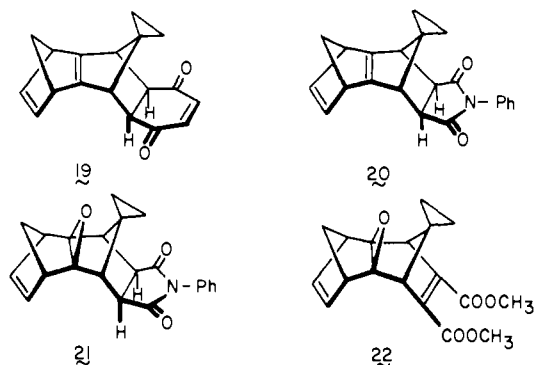
Table II. Selected ^{13}C Chemical Shifts in the Cycloadducts Derived from **3** (ppm, CDCl_3 Solution)^a

compd	C_2', C_3'	C_{12}'	C_{11}'	$\text{C}_8', \text{C}_{10}'$
23	25.05	53.65	81.27	53.65
24	25.05	53.16	81.13	52.77
25	25.06	53.22	74.58	55.71
28	25.44	50.10	76.58	66.25
29	25.15	55.30	75.64	30.93

^a See formula 6 for numbering scheme.

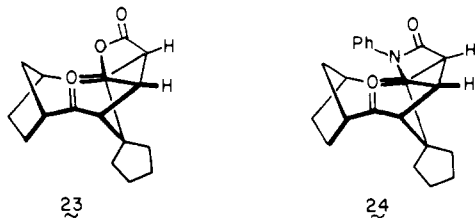
$\text{H}12'_x$ as well as H_2 and H_3 in **17** relative to **16** testify to their mutual close proximity to the epoxide ring.¹³

4',7'-Dihydrospiro[cyclopropane-1,2'-[4,7]methano[2H]indene] (**2**). When **2** was admixed with *p*-benzoquinone, *N*-phenylmaleimide, and dimethyl acetylenedicarboxylate, a single adduct was formed in each case (^1H and ^{13}C NMR analysis). Proof of below-plane dienophile capture was gained in each instance by catalytic hydrogenation to previously isolated adducts of established stereochemistry. By such a reductive procedure, **19** and **20** were transformed into **5** and **13**, respectively. Although the



added double bond in **2** clearly does not disturb the course of kinetically favored stereoselection, its presence does cause the adducts to be rather susceptible to air oxidation. Thus, during product purification by thin-layer chromatography, epoxides **21** and **22** were invariably produced. In the latter case, the third double bond promotes reactivity to such a heightened level that the epoxide alone was isolated. The individual reductive conversion of these compounds to **15** and **17** served as the basis for their structural assignments. Like **1**, therefore, **2** enters into (4 + 2) cycloaddition reactions with very high stereoselectivity from the below-plane direction.

4',5',6',7'-Tetrahydrospiro[cyclopentane-1,2'-[4,7]methano-[2H]indene] (**3**). On standing with maleic anhydride or *N*-phenylmaleimide in benzene solution at 20 °C for several days, **3** was not completely consumed. Nonetheless, it was clear from the ^1H and ^{13}C NMR spectra of the reaction mixtures that adducts **23** and **24** had been formed exclusively in these reactions. The



endo orientation of the heterocyclic rings was deduced principally on the basis of the 3-Hz coupling constant observed to exist between $\text{H}8'_a/\text{H}10'_a$ and the neighboring bridgehead protons. Their further stereochemical designation as *anti*-sesquinorbornene

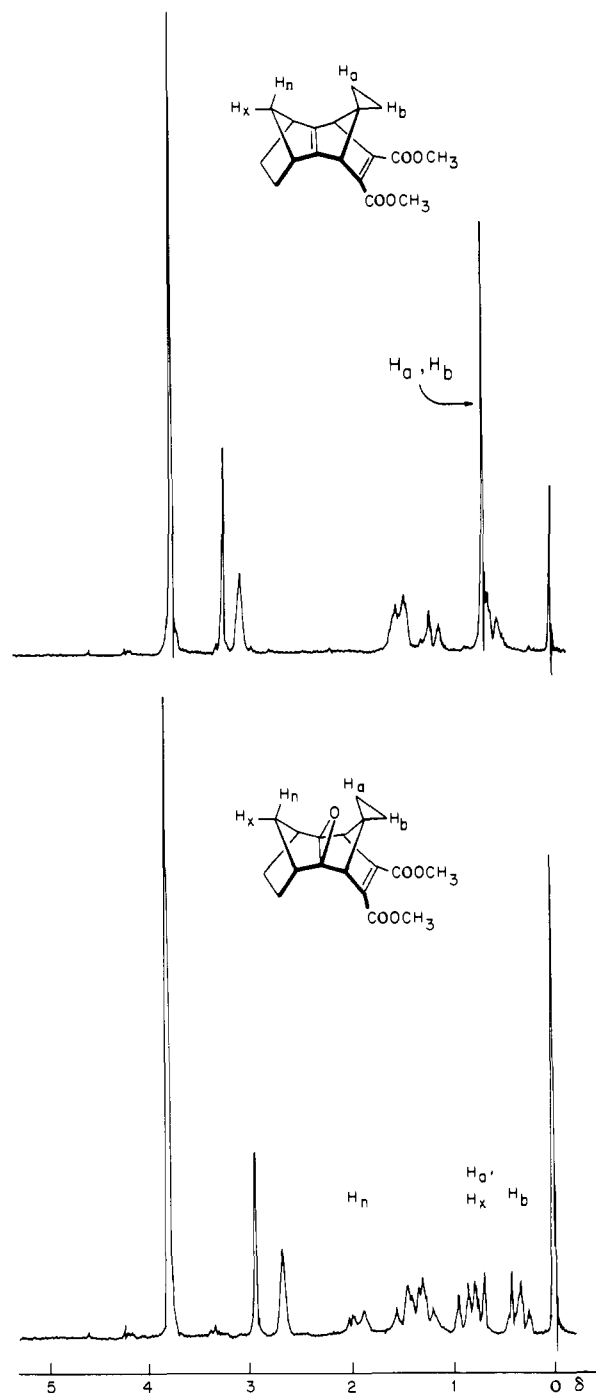
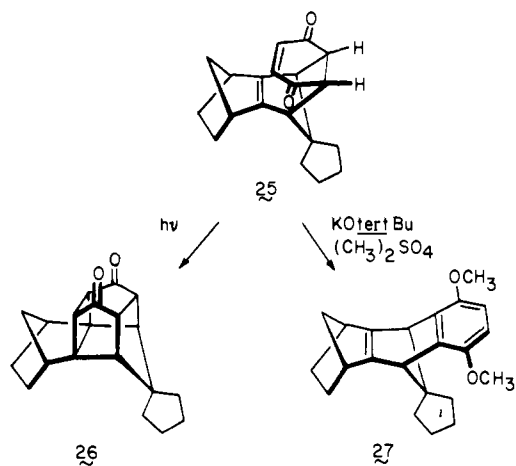


Figure 3. ^1H NMR spectra of adduct **16** (top) and its monoepoxide **17** (bottom) (90 MHz, CDCl_3 , Me_4Si as internal standard).

derivatives follows convincingly from several observations: (a) neither **23** nor **24** is epoxidized by *m*-chloroperbenzoic acid, in contrast to the usual receptiveness of *syn*-sesquinorbornenes toward oxirane formation across their central π bond; (b) the signals for $\text{C}12'$ in these adducts appear in that region which is more typical of **11** than of **10** (Table II); and (c) the ^{13}C NMR spectra of **23** and **24** compare remarkably closely at key positions to that of **25** whose three-dimensional structure has been rigorously established (see below).

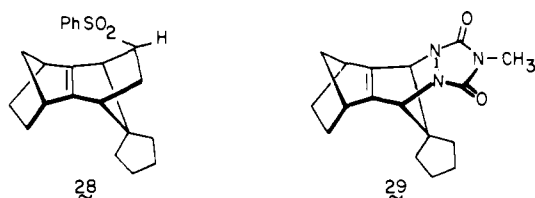
With *p*-benzoquinone as the dienophile, the single adduct **25** was obtained. Due to the structural components present in this molecule, its endo configuration could be established by chemical methods, viz., photocyclization to **26**. In an effort to unravel the additional topological features, its oxygenated ring was aromatized by means of simple O-methylation. Notwithstanding the symmetry of **27**, the anisotropy effects introduced by the benzene ring could not be used to advantage. Therefore, recourse was ultimately

(13) Paquette, L. A.; Fristad, W. E.; Schuman, C. A.; Beno, M. A.; Christoph, G. G. *J. Am. Chem. Soc.* 1979, 101, 4645 and references cited therein.



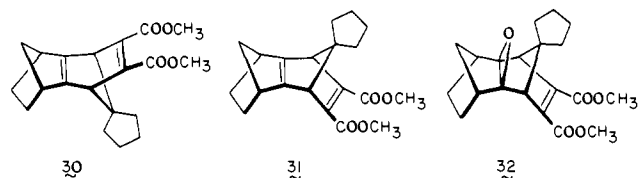
made to X-ray crystal structure analysis (Figure 4).

Similarly, phenyl vinyl sulfone and *N*-methyltriazolinedione added to **3** with high above-plane stereoselectivity to give the adducts **28** and **29**. In order to remove any ambiguity concerning



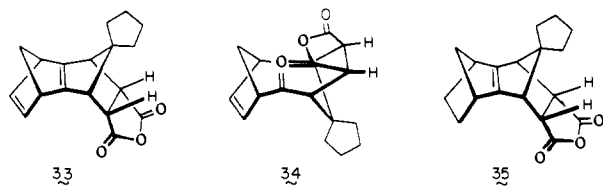
the direction of entry of the most reactive dienophile examined, the single-crystal X-ray structure of **29** was determined. Its *anti*-sesquinorborene character was thereby unequivocally proven (Figure 5).

To provide a further basis of comparison, we conducted a final cycloaddition experiment with DMAD and made the unexpected discovery that two adducts were formed in a 75:25 ratio. There was no doubt that the minor product (**30**) arose by above-plane



attack, since its C12' signal appears at 55.15 ppm and the substance proved unreactive toward *m*-chloroperbenzoic acid. In contrast, the syn stereochemistry of more dominant isomer **31** follows from its higher field C12' chemical shift (48.11 ppm) and its ready peracid oxidation to **32**. Evidently, the involvement of a highly reactive acetylenic dienophile in bonding to **3** leads to a falloff in stereoselectivity. Subsequent work has shown this not to be an uncommon phenomenon.⁶

4',7'-Dihydrospiro[cyclopentane-1,2'-[4,7]methano[2H]indene] (**4**). The reaction of maleic anhydride with **4** proceeded smoothly, although slowly, to give an inseparable mixture of **33** and **34** in



a ratio of 34:66. Conventional ¹H NMR analysis showed the anhydride rings to be endo oriented in both systems. Although the ¹³C NMR profile of the mixture was suggestive of overall molecular architecture, the data were hardly conclusive (Table III). Consequently, the adducts were subjected to catalytic hydrogenation and the dihydro derivatives were spectroscopically

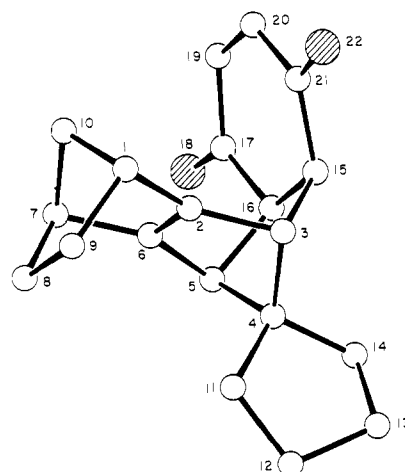


Figure 4. A computer-generated perspective drawing of the final X-ray model of **25** (hydrogens are omitted for clarity).

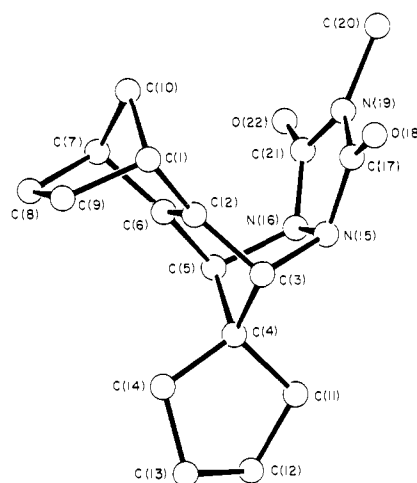


Figure 5. A computer-generated perspective drawing of the final X-ray model of **29** (hydrogens are omitted for clarity).

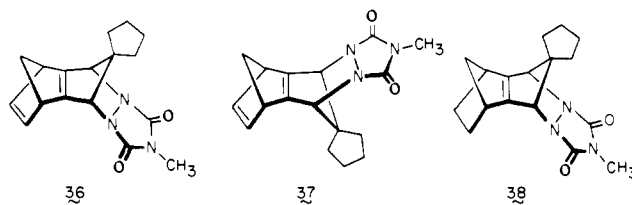
Table III. Selected ¹³C Chemical Shifts in the Maleic Anhydride Adducts Derived from **3** and **4** (ppm, CDCl₃ Solution)^a

compd	C ₂ ', C ₃ '	C ₁₂ '	C ₁₁ '	C ₈ ' _a , C ₁₀ ' _a
33	143.75	77.24	80.45	47.53
34	143.37	77.10	82.92	47.53
35	25.54	55.98	82.63	55.35
23	25.05	53.65	81.27	53.65

^a See formula 6 for numbering scheme.

differentiated. Since the major component proved identical with **23**, the less dominant isomer was necessarily **35**. The ¹³C NMR spectral data for **23** and **35** (Table III) show the major distinguishing feature to be the C11' chemical shift, with that for **35** appearing downfield of that for **23**. We attribute this phenomenon to the endo,*syn* geometry of **35** for which there are few correlatable models.

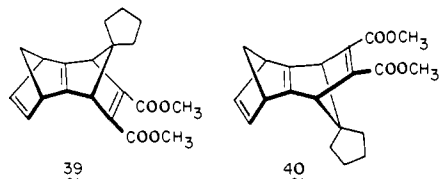
When subjected to analogous treatment with *N*-methyltriazolinedione, **4** underwent ready conversion to a 61:39 mixture of **36** and **37**. During attempts to achieve chromatographic



separation, **37** was selectively destroyed. Isomer **36** was thereby

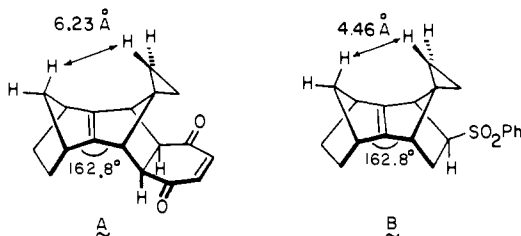
isolated in pure form. Its catalytic hydrogenation delivered the previously unknown urazole **38**. When the cycloadduct mixture was hydrogenated prior to chromatography, the dihydro derivatives **38** and **29** were isolated and their separation offered no difficulty. Particularly satisfying in the ^{13}C NMR spectra of this last pair of isomers were the chemical shifts of C12' and C11'. As expected from earlier precedent, the signals due to syn derivative **38** (52.72 and 75.01 ppm) appear upfield of their counterparts in anti derivative **29** (55.30 and 75.64 ppm).

Where DMAD was concerned, a 78:22 mixture of **39** and **40**



was produced. Following direct spectral analysis of the reaction mixture, these air-sensitive compounds were hydrogenated at atmospheric pressure. Subsequent chromatographic separation afforded **31** (major) and **30** (minor) whose spectra were superimposable upon the samples isolated earlier.

Bond Deformation in the Adducts. The X-ray crystal analyses reported herein (Figures 1, 2, 4, and 5) provide interesting structural information in addition to establishing cycloaddition stereoselectivity. For example, the central double bonds in **5** and **7** share in common the feature of deviating significantly from planarity. As shown in A and B, these torsion angles amount to



a 17.2° distortion from planarity, with tilting occurring in the endo sense. The precision of these data is $\pm 2-3^\circ$. This phenomenon has been encountered previously with *syn*-sesquinorbornenes^{12,14-16} and somewhat simpler norbornenes^{17,18} and has received a modicum of theoretical attention.¹⁹⁻²¹ Steric repulsion cannot be the cause of these molecular deformations since the shortest intramolecular hydrogen-hydrogen distances on the upper faces of these compounds are much greater than normal van der Waal's contacts.

In contrast, adducts **25** and **29** show no such distortion, the observed dihedral angles (2.1 and 0.2°) being within reasonable experimental error of 180° . Of course, there is no a priori reason to believe that these angles must be *exactly* 180° since small deviations from perfect planarity are frequently encountered. Other *anti*-sesquinorbornenes exhibit comparable structural features.^{1,6,15}

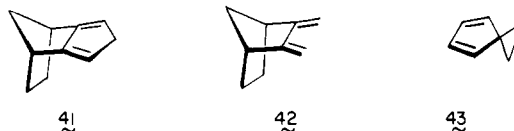
Theoretical and Photoelectron Spectroscopic Analysis of 1 and 3. Our recent studies of systems having nonorthogonal σ and π orbitals have revealed that the high-lying valence orbitals which are predominantly π in character contain significant contributions from the σ frame.^{1,9,12,18} As the result of nonvanishing coupling terms between the pure π and σ orbitals, the resulting canonical one-electron functions are rotated with respect to the molecular plane. Unequal frontier electron densities materialize on the two sides of the π plane. Where various diene derivatives^{1,9,12,18} and naphthalenes fused to a neighboring bicyclic ring system²² are concerned, we have shown that the predominant interaction guiding their stereochemical behavior resides in the destabilizing interaction between the occupied symmetrical π_s molecular orbital of the diene and the symmetrical donor level of the dienophile. As a result of this antibonding interaction, cycloaddition occurs from the face of the π network where interaction between the two doubly occupied molecular orbitals (π_s of diene and π of dienophile) is smallest. Explicit calculation of the four-electron destabilization energy, ΔE (eq 1),^{23,24} yielded energy differences of

$$\Delta E_{ij} = \frac{4(\epsilon_{ij}S_{ij} - H_{ij}S_{ij})}{1 - S_{ij}^2} \quad (1)$$

4–20 kJ/mol for the two competing pathways.⁹ In eq 1, the expression S_{ij} represents the group overlap integral between the two fragment π MO's (π_s of diene and π of dienophile) and the term ϵ_{ij} stands for the average of their one-electron energies ϵ_i and ϵ_j . In addition, H_{ij} represents the interaction matrix element between the fragment MO's i and j .⁹

The structural relationship of **1** and **3** to other recently examined 2,3-dimethylenenorbornane derivatives leads to the expectation that a similar explanation should pertain here. Nonetheless, the key step in any theoretical analysis is to find a computational scheme which delivers an adequate description of the properties of the valence orbitals. The shape and amplitude of canonical π orbitals are presently recognized to be critically dependent on the ordering of the various fragment orbitals. A molecular orbital method that predicts σ orbitals at energies which are too high often arrives at the opposite conclusion concerning the shape of the π MO and is clearly unreliable for the determination of σ/π separations. To test the predictive capability of the available semiempirical MO procedures, we have compared the calculated orbital energies (ϵ_j) with measured vertical ionization potentials ($I_{v,j}$) as obtained from He I photoelectron (PE) spectra.²⁵

Interpretation of the PE spectra assumes Koopmans' approximation²⁶ ($I_{v,j} = -\epsilon_j$) to be valid. Consequently, the canonical orbital energies have been set equal to the negative of the measured vertical ionization potentials. For the derivation of the ϵ_j values, use has been made of the MINDO/3 method²⁷ as well as a recently developed INDO procedure²⁸ successfully applied in our recent studies. To arrive at unambiguous assignments to the PE bands of **1** and **3**, appropriate comparison has been made with the vertical ionization potentials recorded previously for the related systems **41**,⁹ **42**,²⁹ and **43**.³



(14) Paquette, L. A.; Carr, R. V. C.; Charumilind, P.; Blount, J. F. *J. Org. Chem.* **1980**, *45*, 4922.

(15) Watson, W. H.; Galloy, J.; Bartlett, P. D.; Roof, A. A. M. *J. Am. Chem. Soc.* **1981**, *103*, 2022.

(16) Hagenbuch, J.-P.; Vogel, P.; Pinkerton, A. A.; Schwarzenbach, D. *Helv. Chim. Acta* **1981**, *64*, 1819.

(17) Pinkerton, A. A.; Schwarzenbach, D.; Stibbard, J. H. A.; Carrupt, P.-A.; Vogel, P. *J. Am. Chem. Soc.* **1981**, *103*, 2095.

(18) Paquette, L. A.; Schaefer, A. G.; Blount, J. F.; Böhm, M. C.; Gleiter, R. *J. Am. Chem. Soc.*, in press.

(19) (a) Inagaki, S.; Fukui, K. *Chem. Lett.* **1974**, 509. (b) Inagaki, S.; Fujimoto, H.; Fukui, K. *J. Am. Chem. Soc.* **1976**, *98*, 4054.

(20) (a) Wipff, G.; Morokuma, K. *Tetrahedron Lett.* **1980**, 4445. (b) Gleiter, R.; Spanget-Larsen, J. *Ibid.* **1982**, 927. (c) Spanget-Larsen, J.; Gleiter, R. *Ibid.*, in press.

(21) (a) Rondan, N. G.; Paddon-Row, M. N.; Caramella, P.; Houk, K. N. *J. Am. Chem. Soc.* **1981**, *103*, 2436. (b) Caramella, P.; Rondan, N. G.; Paddon-Row, M. N.; Houk, K. N. *Ibid.* **1981**, *103*, 2438.

(22) Paquette, L. A.; Bellamy, F.; Böhm, M. C.; Gleiter, R. *J. Org. Chem.* **1980**, *45*, 4913.

(23) Epiotis, N. D.; Cherry, W. R.; Shaik, S.; Yates, R. L.; Bernardi, F. *Top. Curr. Chem.* **1977**, *70*, 1.

(24) (a) Epiotis, N. D.; Yates, R. L. *J. Am. Chem. Soc.* **1976**, *98*, 461. (b) Baird, N. C.; West, R. H. *Ibid.* **1971**, *93*, 4427. (c) Müller, K. *Helv. Chim. Acta* **1970**, *53*, 1112.

(25) Brundle, C. R.; Baker, A. D. "Electron Spectroscopy: Theory, Techniques, and Applications" Academic Press: London, 1976.

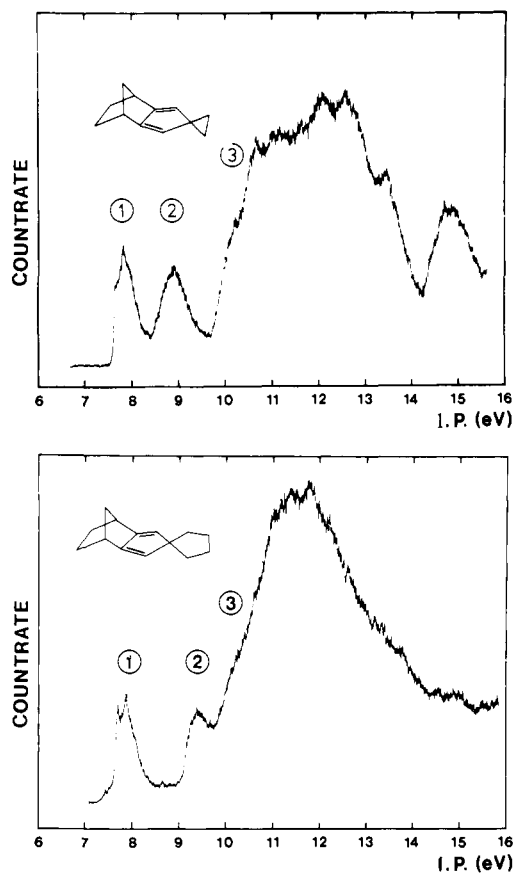
(26) Koopmans, T. *Physica (The Hague)* **1934**, *1*, 104.

(27) (a) Bingham, R. C.; Dewar, M. J. S.; Lo, D. H. *J. Am. Chem. Soc.* **1975**, *97*, 1285. (b) Bischof, P. *Ibid.* **1976**, *98*, 6844.

(28) Böhm, M. C.; Gleiter, R. *Theor. Chim. Acta* **1981**, *59*, 127, 153.

Table IV. Comparison between Measured Vertical Ionization Potentials ($I_{v,j}$) and Calculated Orbital Energies (ϵ_j) according to INDO and MINDO/3 for **1**, **3**, and **41–43** (All Values in eV)

compd	band	$I_{v,j}$	assignment	INDO	MINDO/3
1	1	7.83	π_a	-9.76	-8.56
	2	8.91	(π_s - Walsh)	-10.01	-8.93
	3	10.07 sh	σ	-10.92	-9.55
3	1	7.82	π_a	-8.63	-8.63
	2	9.40	π_s	-10.21	-9.53
	3	10.10 sh	σ	-10.67	-9.67
41	1	7.96	π_a	-9.76	-8.60
	2	9.68	π_s	-10.27	-9.80
	3	10.64	σ	-10.79	-9.67
42	1	8.41	π_a	-10.33	-8.96
	2	10.20	π_s	-11.34	-10.45
	3	10.70	σ	-11.55	-10.01
43	1	8.14	π_a		-8.60
	2	9.46	(π_s - Walsh)		-9.34
	3	10.90	σ		-10.18

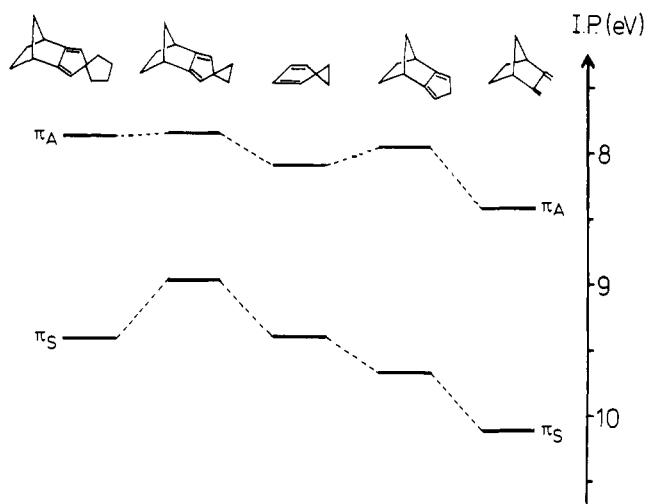
Figure 6. He I PE spectra of **1** and **3**.

The He I PE spectra of **1** and **3**, which are displayed in Figure 6, both show two resolved bands separated by about 0.8 eV from a series of strongly overlapping bands. A third band emerges as a shoulder around 10.1 eV. The ionization potentials are collected in Table IV. Comparison of the first three ionization events within **1** and **3** indicates that bands 1 and 3 are found at comparable energies, while band 2 is shifted toward lower energy in **1** (8.9 eV) relative to **3** (9.4 eV).

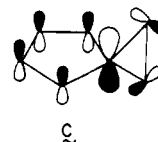
A correlation of the first two ionization potentials of **1** and **3** with those of **41–43** is given in Figure 7. In considering first the PE spectrum of **42**, we see that the first two bands which appear at 8.41 and 10.20 eV have been assigned to the antisymmetric (π_a) and symmetric (π_s) linear combinations of the π orbitals in the butadiene moiety. The effect of the methylene bridge in **41** is to lower both ionization potentials by approximately 0.5 eV. In **43**, the second band, assigned to ionization from the π_s level,

Table V. AO Amplitudes of the Canonical π Orbitals at the Olefinic Carbons in **1** and **3** according to INDO

MO type	1		3
	(π_s - Walsh)	(π_s + Walsh)	π_s
P_i	19a'	13a'	23a'
Γ_j , eV	-10.01	-13.66	-10.21
terminal carbons			
s	-0.0076	0.0144	-0.0109
P_x	0.0187	-0.0998	0.0225
P_y	0.0106	-0.0647	0.0196
P_z	0.3210	0.2463	0.3712
internal carbons			
s	0.0169	-0.0658	0.0227
P_x	-0.0169	0.1255	-0.0190
P_y	-0.0344	0.1141	-0.0574
P_z	0.3974	0.2083	0.4249

Figure 7. Correlation of the first two bands in dienes **1**, **3**, and **41–43**.

is further destabilized due to conjugative interaction with the symmetric Walsh orbital³⁰ of the three-membered ring as shown in C. Similar strong interactions between the π system of a double



bond or a butadiene unit and a cyclopropane ring have been previously noted in various hydrocarbons.^{4,5}

(29) Asmus, P.; Klessinger, M. *Tetrahedron* **1974**, *30*, 2477.(30) (a) Walsh, A. D. *Nature (London)* **1947**, *159*, 167, 712. (b) Walsh, A. D. *Trans. Faraday Soc.* **1949**, *45*, 179. (c) Coulson, C. A.; Moffitt, W. *E. Philos. Mag.* **1949**, *40*, 1.

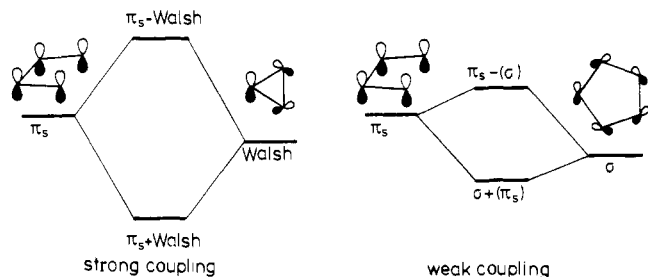


Figure 8. Qualitative interaction diagram between π_s of the diene moiety and the fragment MO of π symmetry located in the cyclopropane (**1**) and cyclopentane rings (**3**).

Suitable comparison of the first two PE bands of **41**–**43** with those of **1** and **3** clearly indicates the first two ionization events in the latter hydrocarbons to be due to ejection from the π_a and π_s orbitals of the butadiene segment. The strong shift of the second band toward lower energy in **1** can be attributed to strong interaction with a cyclopropane Walsh-type orbital as before.

Close examination of Table IV will show that the experimental sequence of the ionization potentials, i.e., π_a and π_s on top of the highest σ orbital, is correctly predicted in all instances only by the INDO technique.

The resulting symmetrical canonical π MO in **1** and **3** can be constructed in two steps. In the first, the pure π orbital of the diene is allowed to interact with the σ frame of the spirocyclic ring. Subsequently, the resulting orbitals are permitted to interact with the remaining σ framework.

According to eq 2, the pure π_s wave functions ($\phi(\pi_s)$) and $\phi(\pi_s C)_\pm = C_1 \phi(\pi_s) \pm C_2 \phi(C)$ (2)

fragment orbital of the conjugative moiety (ϕ_C) are combined into the near-diagonal one-electron function $\phi(\pi_s, C)_\pm$. Due to the π/σ nonorthogonality, both functions [$\phi(\pi_s, C)_+$ and $\phi(\pi_s, C)_-$] interact with the σ ribbon orbitals leading to the wave functions defined in eq 3 and 4. The shapes of the canonical orbitals ϕ_{CMO} are

$$\phi_{CMO+} = \phi(\pi_s, C)_+ + \sum_j \frac{H_{\pi_s, C+j}}{\epsilon_{\pi_s, C+} - \epsilon_{ij}} \phi_j \quad (3)$$

$$\phi_{CMO-} = \phi(\pi_s, C)_- + \sum_j \frac{H_{\pi_s, C-j}}{\epsilon_{\pi_s, C-} - \epsilon_{ij}} \phi_j \quad (4)$$

the result of interaction between $\phi(\pi_s, C)_\pi$ and the σ ribbon orbitals ϕ_j . The magnitudes of π/σ interaction depends on the interaction parameters H_{ij} ($i = \pi_s, C_\pi$) and the energy denominator. It is seen that the sign of the energy differences ($\epsilon_{\pi_s, C+} - \epsilon_{ij}$) and ($\epsilon_{\pi_s, C-} - \epsilon_{ij}$) determines the phase relationship of the π/σ coupling, e.g., the deformation of the canonical MO's of π type.

In Figure 8, the prevailing interactions between the diene moiety and the Walsh-type orbital of the three- and five-membered rings in **1** and **3** are shown in schematic form. For **3**, the corresponding basis orbital energies are about 0.8 eV apart (–10.2 eV for the π_s orbital²⁹ and –11 eV for the σ ribbon orbital³¹) and thus the resulting interaction is predicted to be small. The linear combination $\phi(\pi_s, C)_+$ is therefore mainly a σ orbital, while the $\phi(\pi_s, C)_-$ combination is essentially the π_s orbital admixed to a small extent with an antibonding Walsh-type orbital of the five-membered ring. As concerns **1**, the difference between the basis orbital energies of π_s (–10.2) and of the Walsh-type orbital (–10.7 eV³) is clearly smaller than in **3**. Assuming a resonance integral $H_{\pi_s, C} = -1.15$ eV, one obtains the secular determinant given below,

$$\begin{vmatrix} -10.20 - \epsilon & -1.15 \\ -1.15 & -10.70 - \epsilon \end{vmatrix} = 0 \quad (5)$$

which in turn yields the following eigenvalues and eigenfunctions:

$$\begin{aligned} \phi(\pi_s, C)_+ &= 0.63\phi(\pi_s) + 0.78\phi(C) & \epsilon_+ &= -11.63 \text{ eV} \\ \phi(\pi_s, C)_- &= 0.788\phi(\pi_s) - 0.63\phi(C) & \epsilon_- &= -9.28 \text{ eV} \end{aligned}$$

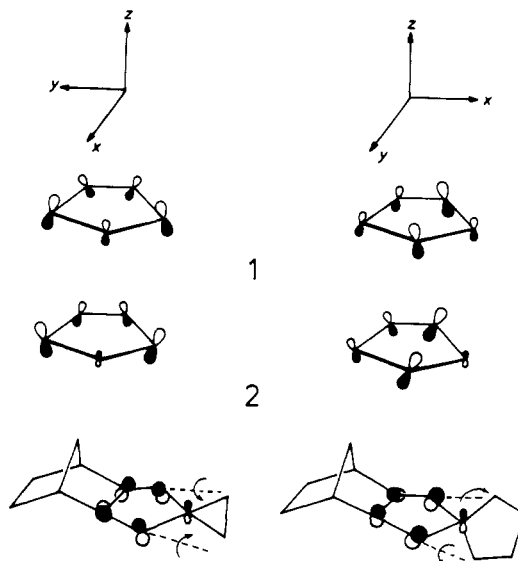


Figure 9. Schematic representation of the bonding linear combinations ($\pi_s + \text{Walsh}$) of **1** and the π_s MO of **3**.

In the resultant wave functions, orbitals $\phi(\pi_s)$ and $\phi(C)$ both contribute about equally. The orbital energy of the antibonding combination (ϵ_-) is well separated from the basis set and hence only a weak interaction as per eq 4 is to be expected. The orbital energy ϵ_+ , however, is close in magnitude to the σ ribbon orbitals and thus a strong interaction between $\phi(\pi_s, C)_+$ and the σ ribbon orbitals is to be expected.

The atomic orbital contributions to the terminal and internal olefinic centers have been calculated for the bonding and antibonding π/Walsh linear combinations of **1** and the π_s molecular orbital of **3** by the INDO procedure. Although π/σ interaction is of little importance in the $\pi_s - \text{Walsh}$ linear combination (19a') of **1**, this phenomenon looms somewhat larger in the π_s orbital (23a') of **3** and is of greatest importance in the $\pi_s + \text{Walsh}$ linear combination (13a') of **1**. Schematic representations of the π_s MO of **3** and the bonding combination of **1** (13a') are given in Figure 9. The terminal π lobes of **3** are instantly recognized to be disrotatorily rotated away from the methano bridge. Superimposed upon this tilting is a second one in the x/z plane wherein the terminal lobes are rotated outwardly from the apical CH_2 , while the $2p_z$ lobes of the internal carbons are skewed inwardly. These opposed deformations in **1** conform to predictions arrived at by the INDO method.

On the basis of Figure 9, antibonding interaction between the diene system and an attacking dienophile should be minimized if the dienophile enters below plane in the case of **1** and above plane in the case of **3**. For both of these approaches, the four-electron destabilization energy is minimized. As the wave functions of **1** and **3** are similar to the canonical orbitals of predominant π character which were discussed by us recently,⁹ the alternative stereoselection schemes are expected to be energetically disfavored by approximately 10–20 kJ/mol.

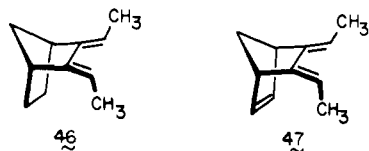
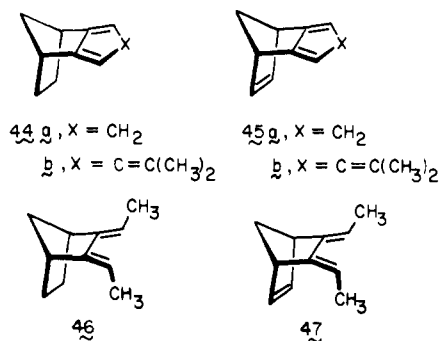
Discussion

The overwhelming kinetic preference for below-plane attack on **1** and **2** by dienophiles of greatly varied reactivity mirrors exactly our earlier findings with **44b** and **45b**.¹² Parent hydrocarbons **44a** and **45a** also follow this trend closely, small levels of above-plane bonding occurring only when maleic anhydride^{9,10} and singlet oxygen³² are involved. This particular π -facial stereoselectivity is likewise adopted by **46** and **47**, except where highly reactive dienophiles are concerned.¹⁸

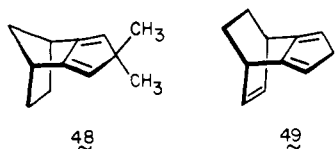
In contrast, the predilection of **3** and **4** for Diels–Alder bonding from above the diene plane parallels the behavior exhibited by

(31) "Handbook of Spectroscopy"; Robinson, J. W., Ed.; CRC Press: Cleveland, OH, 1974; Vol. I.

(32) Paquette, L. A.; Carr, R. V. C.; Arnold, E.; Clardy, J. J. *Org. Chem. Soc.* **1980**, *45*, 4907.



48⁶ and **49**.^{9,14} These systems share in common the additional

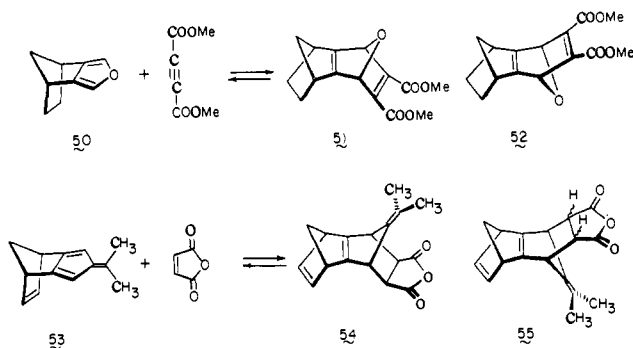


interesting trait that highly reactive dienophiles such as dimethyl acetylenedicarboxylate and *N*-methyltriazolinedione prefer below-plane stereoselectivity and generate products whose topologies differ from these obtained with less reactive dienophilic reagents.

It now becomes relevant to inquire whether these differing stereochemical responses can be attributed to a single cause. In view of the fact that the dienes examined belong to point group C_2 , it appears most likely that symmetry-allowed one-step processes are involved, particularly when the dienophile is also symmetric. Furthermore, the particular electronic relationship of our dienes and dienophiles conforms to the type I classification³³ wherein the $HOMO_{diene} - LUMO_{dienophile}$ energy gap is most important and dominates the reactivity. In other words, electron-releasing substituents in the diene and/or electron-withdrawing substituents in the dienophile should prove effective in enhancing reactivity; indeed, such observations have been made. When reactivity differences can be attributed solely to modifications of frontier orbital energies, perturbation theory suggests that the earlier the transition state, the more clearly will prevailing orbital interactions be made apparent.³⁴

In practice, there are at least four phenomena that could seriously becloud the overall influence of electronic factors. These are as follows:

(a) The possibility that the cycloaddition reactions in question are reversible. Although certain Diels–Alder processes are well-known to be exceptionally prone to reversibility, this behavior is not universally adopted. In actuality, all attempts to detect reversibility and to observe equilibration of norbornyl-fused dienes with their cycloadducts have failed except in the cases of **50** and **53** where, because of the aromaticity of the furan and fulvene ring



systems, conversion to **51** and **54** occurs reversibly at room tem-

(33) Sauer, J.; Sustmann, R. *Angew. Chem., Int. Ed. Engl.* **1980**, *19*, 779.

(34) (a) Sustmann, R. *Tetrahedron Lett.* **1971**, 2717, 2721. (b) Sustmann, R. *Pure Appl. Chem.* **1974**, *40*, 569.

perature.¹⁶ Notwithstanding, no **52** or **55** was found even after long reaction times, thus suggesting either that the same stereoselectivity is achieved irrespective of kinetic or thermodynamic control or that thermodynamic control is not attainable under the conditions employed. Accordingly, it would appear that reversibility may not be a significant factor under the relatively mild conditions utilized in our studies.

(b) The likelihood that steric factors, present in certain dienes and not others, may retard selected reaction rates to such an extent that a slower cycloaddition process having different stereochemical consequences becomes more favorable in these circumstances. However, as kinetic studies reported elsewhere reveal,⁶ **1**, **3**, and **45a** exhibit comparable reactivity toward DMAD (5 times slower than **44a**) whereas **44b** is 55 times less reactive. Thus, the crossover in π -facial stereoselectivity observed for **1** and **3** does not appear to reside in gross kinetic imbalances.³⁵

(c) Changes in transition-state timing may not be a sensitive probe of subjacent orbital tilting effects. The concept of variable transition states has been extensive application in explaining the properties of organic reactions,^{36–43} although invariant selectivity has on occasion accompanied large changes in reactivity.^{44–47} Consequently, it is quite possible that selectivity may sometimes be an insensitive probe of transition-state structure, although its general importance to this question cannot be underestimated. In the present circumstances, the enhanced exothermicity which generally accompanies the reactions of energetic dienophiles is believed to be consistent with early transition states in which bond making between diene and dienophile is less advanced than in slower cycloaddition processes.⁴⁸ However, there persists the lack of a guarantee that such features constitute a sensitive probe of subjacent orbital effects.

(d) A parallelism exists between kinetic and thermodynamic control as the result of fortuitous adherence to the Bell–Evans–Polanyi principle.^{49,50} Under these conditions, the cycloaddition stereoselectivity would be governed by the relative stabilities of the isomeric adducts. This phenomenon is not generally encountered in Diels–Alder chemistry (adherence to the Alder rule,

(35) A referee has suggested that these data do not necessarily rule out a steric origin for the observed changes in stereoselectivity. Because the only substituents that generally lead to above-plane attack are the largest ones examined (*gem*-dimethyl^{6b} and tetramethylene), the concern was oriented toward possible steric control. Thus, the proposed scenario becomes one where the bottom face is inherently more reactive owing to orbital tilting, but becomes too crowded when bulky substituents are attacked, except when DMAD is involved. We find no reason to discount our kinetic data^{6b} and furthermore fail to comprehend how symmetrical substitution above and below plane as in **1**, **3**, and **48** might accelerate bonding to one face more than the other. Rather, the proposed changeover in orbital tilting provides a single explanation for a single phenomenon.

(36) (a) Jencks, D. A.; Jencks, W. P. *J. Am. Chem. Soc.* **1977**, *99*, 7948.

(b) Young, P. R.; Jencks, W. P. *Ibid.* **1979**, *101*, 3288.

(37) (a) Thornton, E. R. *J. Am. Chem. Soc.* **1967**, *89*, 2915. (b) Winey, D. A.; Thornton, E. R. *Ibid.* **1975**, *97*, 3102.

(38) Gajewski, J. J.; Conrad, N. D. *J. Am. Chem. Soc.* **1979**, *101*, 6693.

(39) (a) Harris, J. M.; Paley, M. S.; Prasthofer, T. W. *J. Am. Chem. Soc.* **1981**, *103*, 5915. (b) Harris, J. M.; Shafer, S. G.; Moffatt, J. R.; Becker, A. R. *Ibid.* **1979**, *101*, 3295. (c) Shafer, S. G.; Harris, J. M. *J. Org. Chem.* **1981**, *46*, 2164.

(40) Shiner, V. J., Jr.; Seib, R. C. *J. Am. Chem. Soc.* **1976**, *98*, 862.

(41) (a) Bernasconi, C. F. *Acc. Chem. Res.* **1978**, *11*, 147. (b) Bernasconi, C. F.; Gandier, J. R. *J. Am. Chem. Soc.* **1978**, *100*, 8117.

(42) (a) Albery, W. J.; Kreevoy, M. M. *Prog. Phys. Org. Chem.* **1978**, *13*, 87. (b) Albery, W. J. "Progress in Reaction Kinetics"; Pergamon Press: Oxford, 1967; Vol. 4, p 355.

(43) (a) More O'Ferrall, R. A. *J. Chem. Soc. B* **1970**, 274. (b) Bunnett, J. F. *Angew. Chem., Int. Ed. Engl.* **1982**, *21*, 225.

(44) Arnett, E. M.; Reich, R. *J. Am. Chem. Soc.* **1980**, *102*, 5892.

(45) Bordwell, F. G.; Hughes, D. L. *J. Org. Chem.* **1980**, *45*, 3314, 3320.

(46) Koshy, K. M.; Roy, D.; Tidwell, T. T. *J. Am. Chem. Soc.* **1979**, *101*, 357.

(47) (a) Pross, A. *Adv. Phys. Chem.* **1977**, *14*, 69. (b) Giese, B. *Angew. Chem., Int. Ed. Engl.* **1977**, *16*, 125.

(48) (a) Huisgen, R.; Schug, R. *J. Am. Chem. Soc.* **1976**, *98*, 7819. (b) Kiselev, V. D.; Miller, J. G. *Ibid.* **1975**, *97*, 4036.

(49) Dewar, M. J. S.; Dougherty, R. C. "The PMO Theory of Organic Chemistry"; Plenum Press: New York, 1975; p 212.

(50) Avenati, M.; Hagenbuch, J.-P.; Mahaim, C.; Vogel, P. *Tetrahedron Lett.* **1980**, 3167.

The less rapidly eluted component was identified as **14**: 73 mg (12%); mp 170–171 °C; ^1H NMR (CDCl_3) δ 7.50–7.12 (m, 5 H), 3.67 (m, 2 H), 3.00 (m, 2 H), 2.75 (m, 2 H), 1.80–1.55 (m, 2 H), 1.23–1.00 (m, 4 H), 0.45 (s, 4 H); ^{13}C NMR (ppm, CDCl_3) 176.72, 152.35, 132.10, 128.85, 128.07, 126.08, 57.05, 50.25, 49.76, 47.82, 42.33, 25.73, 9.95, 6.31; mass spectrum m/e (M^+) calcd, 331.1572; obsd, 331.1562.

Anal. Calcd for $\text{C}_{22}\text{H}_{21}\text{NO}_2$: C, 79.73; H, 6.39. Found: C, 79.58; H, 6.45.

Peracid Oxidation of 13. To an ice-cold solution of **13** (100 mg, 0.30 mmol) in 15 mL of dichloromethane was slowly added a solution of *m*-chloroperbenzoic acid (78 mg of 80%, 0.36 mmol) in 10 mL of the same solvent. The reaction mixture was stirred at room temperature for 12 days. Although starting material remained (TLC analysis), the solution was washed with sodium thiosulfate solution (50 mL), saturated sodium bicarbonate solution (50 mL), and water (50 mL). The organic layer was dried, filtered, and evaporated, and the residue was purified by TLC on silica gel (elution with 20% ethyl acetate in hexanes). There was obtained 55 mg (53%) of epoxide **15**: mp 206–207 °C; ^1H NMR (CDCl_3) δ 7.60–7.17 (m, 5 H), 3.70 (s, 2 H), 2.93 (br m, 2 H), 2.73 (s, 2 H), 2.15–1.47 (series of m, 5 H), 0.85–0.25 [A_2B_2 from 0.70–0.25 (4 H), total area 5 H]; ^{13}C NMR (ppm, CDCl_3) 117.16, 132.05, 129.29, 128.65, 126.03, 59.23, 50.44, 48.79, 41.27, 38.60, 32.62, 26.99, 8.16, 5.25; mass spectrum, m/e (M^+) calcd, 347.1521; obsd, 347.1528.

Anal. Calcd for $\text{C}_{22}\text{H}_{21}\text{NO}_3$: C, 76.06; H, 6.09. Found: C, 75.72; H, 6.14.

syn-Dimethyl 1',2',3',4',5',6',7',8'-Hexahydrospiro[cyclopropane-1,9'-[1,4:5,8]dimethanonaphthalene]-6,7'-dicarboxylate (16). A solution of **1** (300 mg, 1.90 mmol) and dimethyl acetylenedicarboxylate (400 mg, 2.85 mmol) in chloroform (5 mL) was stirred under nitrogen at room temperature for 4 h. The solvent was evaporated and the lone adduct was purified by preparative TLC on silica gel (elution with 20% ethyl acetate in hexane). There was isolated 400 mg (70%) of **16** as a slightly yellow oil: ^1H NMR (CDCl_3) δ 3.73 (s, 6 H), 3.60 (s, 2 H), 3.03 (br m, 2 H), 1.60–1.03 (m, 4 H), 0.67 (s, 4 H), 0.60–0.46 (m, 2 H); ^{13}C NMR (ppm, CDCl_3) 166.04, 157.98, 150.06, 66.22, 57.53, 51.95, 48.01, 43.01, 22.58, 10.10, 7.96.

A chloroform solution of **16**, upon standing for 2–3 days, was oxidized by air to a mixture of compounds. Separation was achieved by preparative TLC on silica gel (20% ethyl acetate in hexanes elution). First to elute was unoxidized **16** (120 mg, 30%).

The second component was epoxide **17** which was isolated as a slightly yellow oil (82 mg, 14%): ^1H NMR (CDCl_3) δ 3.80 (s, 6 H), 2.93 (s, 2 H), 2.67 (br s, 2 H), 2.07–1.80 (m, 1 H), 1.60–1.10 (m, 4 H), 0.97–0.70 (m, 3 H), 0.47–0.20 (m, 2 H); ^{13}C NMR (ppm, CDCl_3) 165.12, 149.14, 66.27, 55.03, 54.33, 42.29, 39.86, 38.94, 25.00, 14.32, 2.48; mass spectrum, m/e mass at 316 was too small for high accuracy measurement.

The third component proved to be diketone **18**: a white solid (62 mg 10%); mp 157–159 °C (from hexanes); IR (cm^{-1} , KBr) 1687 and 1735; ^1H NMR (CDCl_3) δ 3.83 (s, 6 H), 3.43 (s, 2 H), 3.40–3.13 (m, 2 H), 2.30–2.10 (m, 6 H), 0.83 (s, 4 H); ^{13}C NMR (ppm, CDCl_3) 208.70, 164.10, 140.24, 68.94, 54.13, 52.74, 34.59, 28.04, 27.19, 23.30, 9.71; mass spectrum, m/e (M^+) calcd, 332.1260; obsd, 332.1251.

Anal. Calcd for $\text{C}_{18}\text{H}_{20}\text{O}_6$: C, 65.05; H, 6.07. Found: C, 64.75; H, 6.09.

Peracid Epoxidation of 16. *m*-Chloroperbenzoic acid (253 mg, 1.47 mmol) dissolved in 20 mL of dichloromethane was added to a solution of **16** (400 mg, 1.33 mmol) in the same solvent (20 mL). Reaction occurred rapidly and after 1 h the reaction mixture was worked up as before to afford epoxide **17** in quantitative yield.

Oxygenation of 16. Oxygen was bubbled through a solution of **16** (120 mg, 0.4 mmol) in benzene for 3 days. ^1H NMR analysis of the reaction mixture indicated the ratio of **16**:**17**:**18** to be 45:33:22.

syn-exo-1',4',8'a,9',10',10'a-Hexahydrospiro[cyclopropane-1,11'-[1,4:9,10]dimethanoanthracene]-5',8'-dione (19). A solution of **2** (300 mg, 1.92 mmol) and benzoquinone (420 mg, 3.85 mmol) in 10 mL of chloroform was stirred at room temperature under nitrogen for 2 weeks. TLC analysis indicated a reasonable amount of unreacted starting materials to be present. The solvent was evaporated and the unconsumed reactants were removed by sublimation at 70 °C and 20 torr (2 h). The residue was purified by preparative TLC on silica gel (elution with 15% ethyl acetate in hexane). There was isolated 160 mg (32%) of **19** as the only observable adduct; colorless solid, mp 134.5–135.5 °C (from hexanes); ^1H NMR (CDCl_3) δ 6.68 (s, 2 H), 6.50 (t, $J = 2$ Hz, 2 H), 3.46 (m, 2 H), 2.93 (s, 2 H), 2.30–2.03 (A_2B_2 , 2 H), 2.00 (s, 2 H), 0.60–0.10 (A_2B_2 , 4 H); ^{13}C NMR (ppm, CDCl_3) 200.81, 159.24, 141.46, 138.55, 69.79, 55.35, 48.91, 45.45, 41.75, 8.13, 4.37; mass spectrum, m/e 264 was too small for high accuracy measurement.

Anal. Calcd for $\text{C}_{18}\text{H}_{16}\text{O}_2$: C, 81.79; H, 6.10. Found: C, 81.54; H, 6.12.

Hydrogenation of 19. A stirred solution of **19** (100 mg, 0.38 mmol) in ethyl acetate (5 mL) containing platinum oxide (20 mg) was hydrogenated at atmospheric pressure for 12 min. The product was purified by TLC on silica gel (elution with 20% ethyl acetate in hexanes). There was isolated 62 mg (61%) of **5**, mp 151–152 °C (from hexanes). Admixed melting point with authentic material was undepressed.

syn-exo-1',4',5',6',7',8'-Hexahydro-N-phenylspiro[cyclopropane-1,9'-[1,4:5,8]dimethanonaphthalene]-6',7'-dicarboximide (20). A solution of **2** (300 mg, 1.92 mmol) and *N*-phenylmaleimide (300 mg, 1.73 mmol) in benzene (5 mL) was stirred at room temperature under a nitrogen atmosphere for 8 days. A small amount of insoluble polymer was separated by filtration and the filtrate was evaporated to dryness. The residue was recrystallized from ether to give 230 mg of pale yellow solid which consisted of two compounds in a 4:1 ratio. TLC separation (silica gel; 15% ethyl acetate in hexane) afforded 140 mg (22%) of pure **20** as a colorless oil; ^1H NMR (CDCl_3) δ 7.60–7.10 (m, 5 H), 6.58 (t, $J = 2$ Hz, 2 H), 3.50 (br s, 2 H), 2.96 (2 H), 2.47 (s, 2 H), 2.37–2.05 (A_2B_2 , 2 H), 0.60 (br s, 4 H); ^{13}C NMR (ppm, CDCl_3) 177.50, 161.52, 139.38, 132.25, 129.19, 128.51, 126.23, 70.10, 50.04, 49.13, 47.00, 39.42, 8.20, 2.91; mass spectrum, m/e (M^+) calcd, 329.1416; obsd, 329.1407.

The more polar component proved to be epoxide **21** (110 mg, 17%): mp 189–190 °C (from ether); ^1H NMR (CDCl_3) δ 7.57–7.16 (m, 5 H), 6.50 (br s, 2 H), 3.16 (br s, 2 H), 3.06 (s, 2 H), 2.60 (s, 2 H), 2.15 (d, $J = 7.5$ Hz, 1 H), 1.55 (d, $J = 7.5$ Hz, 1 H), 0.76–0.26 (A_2B_2 , 4 H); ^{13}C NMR (ppm, CDCl_3) 176.86, 139.72, 132.25, 129.19, 128.56, 126.03, 67.24, 53.50, 48.84, 48.16, 45.25, 33.06, 7.38, 4.37; mass spectrum, m/e (M^+) calcd, 345.1365; obsd, 345.1373.

Hydrogenation of 20. A 25 mg (0.076 mmol) sample of **20** was hydrogenated over platinum oxide for 12 min in the prescribed manner. The usual workup afforded **13** whose ^1H and ^{13}C NMR spectra were identical with those of the authentic sample.

Hydrogenation of 21. A 45 mg (0.13 mmol) sample of **21** dissolved in ethyl acetate (10 mL) was hydrogenated for 15 min over platinum oxide as described above. Preparative TLC purification on silica gel (elution with 20% ethyl acetate in hexanes) furnished 35 mg (76%) of **15**, mp 206–207 °C (from hexanes).

syn-Dimethyl 4'a,8'a-Epoxy-1',4',4'a,5',8',8'a-octahydrospiro[cyclopropane-1,9'-[1,4:5,8]dimethanonaphthalene]-6',7'-dicarboxylate (22). A solution of **2** (200 mg, 1.28 mmol) and dimethyl acetylenedicarboxylate (364 mg, 2.56 mmol) in chloroform (30 mL) was heated at the reflux temperature under a nitrogen atmosphere for 6 h. The solvent was evaporated and the excess DMAD was removed in vacuo. Purification of the product was achieved by preparative TLC on silica gel (elution with 30% ethyl acetate in hexanes). There was isolated 47 mg (12%) of epoxide **22** as a faintly yellow oil; ^1H NMR (CDCl_3) δ 6.25 (t, $J = 2$ Hz, 2 H), 3.83 (s, 6 H), 3.13 (br m, 2 H), 2.95 (s, 2 H), 2.18 (d, $J = 7.5$ Hz, 1 H), 1.40 (d, $J = 7.5$ Hz, 1 H), 0.53 (A_2B_2 , 4 H); ^{13}C NMR (ppm, CDCl_3) 164.73, 150.65, 141.28, 75.88, 55.98, 52.09, 51.80, 49.47, 46.02, 13.65, 2.57; mass spectrum, m/e (M^+) calcd, 314.1154; obsd, 314.1161.

Hydrogenation of 22. A solution of **22** (45 mg, 0.14 mmol) in 5 mL of ethyl acetate was hydrogenated over platinum in the prescribed manner. The isolated product proved to be spectroscopically identical (^1H and ^{13}C NMR) to authentic **17** prepared earlier.

anti-endo-1',2',3',4',5',6',7',8'-Octahydrospiro[cyclopentane-1,9'-[1,4:5,8]dimethanonaphthalene]-6',7'-dicarboxylic Anhydride (23). A solution of **3** (300 mg, 1.61 mmol) and maleic anhydride (150 mg, 1.55 mmol) in dry benzene (5 mL) was stirred at room temperature for 4 days. The solvent was removed and the residue was recrystallized from ether to give 160 mg of **23**. The filtrate was evaporated and the residue was subjected to TLC on silica gel (elution with hexanes–ethyl acetate, 9:1). An additional 55 mg of **23** (total 47%) was isolated: mp 102–107 °C; no other adducts were detected spectroscopically; ^1H NMR (CDCl_3) δ 3.70 (m, 2 H), 3.06 (m, 2 H), 2.90 (m, 2 H), 2.00–1.05 (series of m, 14 H); ^{13}C NMR (ppm, CDCl_3) 172.06, 152.78, 81.27, 53.65 (3 C), 48.69, 42.14, 33.50, 31.75, 25.97, 25.05 (3 C); mass spectrum, m/e calcd, 284.1412; obsd, 284.1404.

anti-endo-1',2',3',4',5',6',7',8'-Octahydro-6'-(phenylsulfonyl)spiro[cyclopentane-1,9'-[1,4:5,8]dimethanonaphthalene] (28). A solution of **3** (680 mg, 3.66 mmol) and phenyl vinyl sulfone (610 mg, 3.66 mmol) in toluene (25 mL) was heated at the reflux temperature for 30 days. The solvent was evaporated and the residue was purified by TLC on silica gel. Elution with 15% ethyl acetate in hexanes gave **28** as an oil which solidified when triturated with hexanes. Pure **28** was obtained as colorless crystals, mp 94–95 °C (from hexanes); ^1H NMR (CDCl_3) δ 7.90–7.75 (m, 2 H), 7.60–7.40 (m, 3 H), 3.83–3.53 (m, 1 H), 3.03–2.83 (m, 2 H), 2.60–2.40 (m, 2 H), 2.20–1.93 (m, 2 H), 1.90–1.00 (series of m, 12 H); ^{13}C NMR (ppm, CDCl_3) 154.77, 148.12, 141.33, 133.07, 129.14, 128.02, 76.56, 66.27, 53.26, 52.72, 50.10, 43.11, 41.41, 33.40, 32.09, 30.93, 26.22, 25.78, 25.49, 25.15; mass spectrum, m/e (M^+) calcd, 354.1653; obsd, 354.1648.

Anal. Calcd for $C_{22}H_{26}O_2S$: C, 74.54; H, 7.39. Found: C, 74.56; H, 7.41.

anti-endo-1',2',3',4',8'a,9',10',10'a-Octahydrospiro[cyclopentane-1,11'-[1,4,9,10]dimethanoanthracene]-5',8'-dione (25). A solution of **3** (300 mg, 1.61 mmol) and benzoquinone (260 mg, 2.42 mmol) in chloroform (5 mL) was stirred at 42 °C for 5 days. The solvent was evaporated and the residue was heated in a sublimator at 75 °C and 0.1 torr for 1 h to remove unreacted reactants. The semisolid residue was recrystallized from hexanes to give 309 mg (65%) of **3**, mp 151.5–152.5 °C; 1H NMR ($CDCl_3$) δ 6.60 (s, 2 H), 3.40 (m, 2 H), 3.13 (m, 2 H), 2.73 (br s, 2 H), 1.80–1.00 (series of m, 14 H); ^{13}C NMR (ppm, $CDCl_3$) 199.90, 153.05, 142.31, 74.58, 55.71, 53.22, 50.25, 41.87, 33.56, 31.56, 26.21, 25.25, 25.06; mass spectrum, m/e (M^+) calcd, 294.1620; obsd, 294.1611.

Anal. Calcd for $C_{20}H_{22}O_2$: C, 81.60; H, 7.53. Found: C, 81.43; H, 7.50.

anti-1',2',3',4',9',10'-Hexahydro-5',8'-dimethoxyspiro[cyclopentane-1,11'-[1,4,9,10]dimethanoanthracene] (27). A cold (0 °C), stirred solution of **25** (100 mg, 0.34 mmol) and dimethyl sulfate (128 mg, 1.02 mmol) in dry tetrahydrofuran (20 mL) was treated with three 35-mg portions of potassium *tert*-butoxide at 1-h intervals while under a nitrogen atmosphere. The reaction mixture was stirred overnight at room temperature and filtered through a Celite pad. The filtrate was concentrated and the residue was subjected to preparative TLC on silica gel. Elution with 15% ethyl acetate in hexanes afforded 25 mg (23%) of **27** as a colorless oil which solidified on standing; 1H NMR ($CDCl_3$) δ 6.43 (s, 2 H), 3.77 (s, 6 H), 3.67 (s, 2 H), 3.00 (br s, 2 H), 1.90–1.70 (m, 2 H), 1.57–1.10 (m, 12 H); ^{13}C NMR (ppm, $CDCl_3$) 160.45, 149.14, 142.78, 110.55, 95.11, 57.14, 55.10, 54.81, 42.58, 34.52, 32.92, 25.68, 25.54 (3 C); mass spectrum, m/e (M^+) calcd, 322.1933; obsd, 322.1941.

Photocyclization of 25. A solution of **25** (17 mg, 0.06 mmol) in acetonitrile (3 mL) was placed in a Pyrex test tube and irradiated with a bank of 3500-Å lamps in a Rayonet reactor for 6 h. Evaporation of solvent gave **26** (100%): mp 200–201 °C (from hexanes); 1H NMR ($CDCl_3$) δ 2.93 (m, 2 H), 2.73 (m, 2 H), 2.50–2.20 (m, 4 H), 2.20–1.90 (m, 2 H), 1.80–1.40 (m, 12 H); ^{13}C NMR (ppm, $CDCl_3$) 211.01, 65.48, 57.59, 56.56, 53.71, 48.24, 44.12, 41.93, 38.90, 32.22, 26.40, 25.79, 23.00; mass spectrum, m/e (M^+) calcd, 294.1620; obsd, 294.1611.

Anal. Calcd for $C_{20}H_{22}O_2$: C, 81.60; H, 7.53. Found: C, 81.32; H, 7.58.

anti-1',4',5',6',7',8'-Hexahydro-N-methylspiro[cyclopentane-1,10'-[1,4,5,8]dimethanophthalazine]-2',3'-dicarboximide (29). Into a cold (–78 °C), stirred solution of **3** (187 mg, 1.01 mmol) in ethyl acetate (10 mL) was syringed a solution of *N*-methyltriazolinedione (114 mg, 1.01 mmol) in 10 mL of the same solvent. Upon completion of the addition, the reaction mixture was stirred for 30 min at –78 °C and 30 min at 25 °C. Careful evaporation of the solvent without heating left a solid whose ^{13}C NMR spectrum showed it to be a single isomer. This adduct (175 mg, 55%) was obtained as colorless crystals, mp 158–160 °C dec; 1H NMR ($CDCl_3$) δ 4.50 (s, 2 H), 2.98 (br s, 2 H), 2.90 (s, 3 H), 1.93–1.35 (m, 9 H), 1.33–1.06 (m, 5 H); ^{13}C NMR (ppm, $CDCl_3$) 161.23, 150.60, 75.64, 71.22, 55.30, 41.36, 32.82, 30.93, 26.36, 25.54, 25.34, 24.91.

Anal. Calcd for $C_{17}H_{21}N_3O_2$: C, 68.20; H, 7.07. Found: C, 68.27; H, 7.23.

anti-endo-1',2',3',4',5',6',7',8'-Octahydro-N-phenylspiro[cyclopentane-1,9'-[1,4,5,8]dimethanonaphthalene]-6',7'-dicarboximide (24). A solution of **3** (300 mg, 1.61 mmol) and *N*-phenylmaleimide (270 mg, 1.55 mmol) in benzene (5 mL) was stirred at room temperature under nitrogen for 5 days. TLC analysis at this point showed considerable levels of the starting materials to remain. The solvent was evaporated and the sole adduct was isolated by preparative TLC on silica gel (elution with 10% ethyl acetate in hexanes) and recrystallization from ether: 229 mg (40%), mp 160.5–161.6 °C; 1H NMR ($CDCl_3$) δ 7.43–7.06 (m, 5 H), 3.46 (m, 2 H), 2.95 (m, 2 H), 2.86 (m, 2 H), 1.85–1.03 (m, 14 H); ^{13}C NMR (ppm, $CDCl_3$) 177.01, 151.91, 81.13, 53.16, 52.77, 47.72, 41.99, 33.55, 31.99, 25.97, 25.05 (3 C); mass spectrum, m/e (M^+) calcd, 359.1885; obsd, 359.1877.

Anal. Calcd for $C_{24}H_{25}NO_2$: C, 80.19; H, 7.01. Found: C, 80.21; H, 7.11.

Dimethyl syn- and anti-1',2',3',4',5',8'-Hexahydrospiro[cyclopentane-1,9'-[1,4,5,8]dimethanonaphthalene]-6',7'-dicarboxylates (30 and 31). A solution of **3** (800 mg, 4.30 mmol) and dimethyl acetylenedicarboxylate (670 mg, 4.73 mmol) in chloroform (50 mL) was stirred at room temperature for 5 h. The solvent was evaporated and the oily residue was separated into its two components by medium-pressure liquid chromatography on silica gel. Elution with 10% ethyl acetate in hexane afforded 950 mg (67%) of **31** and 300 mg (21%) of **30**.

For **31**: colorless crystals, mp 75–76 °C (from hexanes); 1H NMR ($CDCl_3$) δ 3.77 (s, 6 H), 3.46 (s, 2 H), 3.00 (br s, 2 H), 1.85–1.27 (m, 12 H), 0.60–0.40 (m, 2 H); ^{13}C NMR (ppm, $CDCl_3$) 166.47, 158.12,

149.92, 93.94, 61.17, 51.95, 48.11, 42.97, 34.37, 32.72, 25.49, 25.10, 22.67; mass spectrum, m/e (M^+) calcd, 328.1674; obsd, 328.1666.

Anal. Calcd for $C_{20}H_{24}O_4$: C, 73.15; H, 7.36. Found: C, 73.16; H, 7.37.

For **30**: 1H NMR ($CDCl_3$) δ 3.73 (s, 6 H), 3.46 (s, 2 H), 3.03 (br s, 2 H), 1.95–1.10 (series of m, 14 H); ^{13}C NMR (ppm, $CDCl_3$) 166.13, 160.55, 153.85, 100.30, 61.32, 55.15, 51.85, 42.92, 34.23, 32.82, 25.29; mass spectrum, m/e (M^+) calcd, 328.1674; obsd, 328.1682.

Peracid Oxidation of 31. To a stirred, ice-cold solution of **31** (82 mg, 0.25 mmol) in dichloromethane (10 mL) was added a solution of *m*-chloroperbenzoic acid (64.6 mg, 0.30 mmol) in 10 mL of the same solvent. The reaction mixture was heated at the reflux temperature for 15 h and the epoxide was isolated as before. There was isolated 83 mg (96%) of **32** after TLC on silica gel (elution with 15% ethyl acetate in hexanes); colorless solid: mp 132.5–133.5 °C (from hexanes); IR (cm^{-1} , KBr) 1715; 1H NMR ($CDCl_3$) δ 3.80 (s, 6 H), 3.15 (s, 2 H), 2.60 (br s, 2 H), 1.97–1.17 (series of m, 13 H), 0.90–0.70 (m, 1 H); ^{13}C NMR (ppm, $CDCl_3$) 165.50, 149.43, 81.81, 65.93, 57.77, 52.24, 40.20, 38.60, 37.58, 36.75, 27.92, 25.20, 24.86; mass spectrum, m/e (M^+) calcd, 344.1624; obsd, 344.1629.

Anal. Calcd for $C_{20}H_{24}O_5$: C, 69.75; H, 7.02. Found: C, 69.91; H, 6.96.

syn- and anti-1',4',5',6',7',8'-Hexahydrospiro[cyclopentane-1,9'-[1,4,5,8]dimethanonaphthalene]-6',7'-dicarboxylic Anhydrides (33 and 34). A solution of **4** (200 mg, 1.09 mmol) and maleic anhydride (533 mg, 5.43 mmol) in benzene (20 mL) was stirred at room temperature for 10 days. The resulting cloudy solution was concentrated to dryness and the excess maleic anhydride was removed by sublimation (50 °C (0.05 torr)). The residue was dissolved in chloroform and hexane (25 mL) was added. The white precipitate which formed was separated by filtration and purified by MPLC on silica gel (15% ethyl acetate in hexanes as eluant). The two isomeric adducts (34% of **33** and 66% of **34** by 1H NMR analysis) eluted as a single band (290 mg, 94%). After recording of the ^{13}C NMR spectrum, this mixture was directly hydrogenated.

For *syn* isomer **33**: ^{13}C NMR (ppm, $CDCl_3$) 171.72, 162.11, 143.15, 80.45, 77.24, 54.62, 50.01, 47.53, 32.96, 32.62, 25.93, and 25.15.

For *anti* isomer **34**: ^{13}C NMR (ppm, $CDCl_3$) 172.11, 162.98, 143.37, 82.92, 77.10, 53.94, 50.30, 48.69, 33.21, 25.93, 24.86.

Hydrogenation of Adducts 33 and 34. A solution of the **33/34** mixture (230 mg, 0.81 mmol) in ethyl acetate (10 mL) containing 20 mg of 5% palladium on carbon was hydrogenated at atmospheric pressure for 20 min. The reaction mixture was filtered and evaporated to dryness. The 1H and ^{13}C NMR spectra were then compared with those of the known *exo* isomer **23**. By peak subtraction, the ^{13}C NMR chemical shifts for *endo* isomer **35** were determined to be as follows: (ppm, $CDCl_3$) 172.74, 155.50, 82.63, 55.98, 55.35, 48.16, 43.21, 33.30, 33.11, 25.54, 25.05.

syn- and anti-1',4',5',8'-Tetrahydro-N-methylspiro[cyclopentane-1,10'-[1,4,5,8]dimethanophthalazine]-2',3'-dicarboximides (36 and 37). A cold (–78 °C), stirred solution of **4** (300 mg, 1.63 mmol) in ethyl acetate (30 mL) was treated dropwise with a solution of *N*-methyltriazolinedione (184 mg, 1.63 mmol) in the same solvent (15 mL). After being stirred for 4 h at this temperature, the reaction mixture was evaporated to dryness and the solid residue was analyzed by 1H NMR (ratio of adducts 61:39). MPLC on silica gel (elution with 24% ethyl acetate in petroleum ether) selectively destroyed the *anti* isomer, giving the major *syn* isomer in pure form (42% isolated); colorless oil: 1H NMR ($CDCl_3$) δ 6.50 (t, $J = 2.5$ Hz, 2 H), 4.65 (s, 2 H), 3.56 (br s, 2 H), 2.80 (s, 3 H), 2.23 (m, 2 H), 1.85–1.50 (m, 8 H); ^{13}C NMR (ppm, $CDCl_3$) 160.75, 159.29, 142.73, 74.72, 72.53, 70.20, 48.69, 32.38, 32.14, 26.12, 25.83, 25.15; mass spectrum, m/e (M^+) calcd, 297.1477; obsd, 297.1486.

Catalytic Hydrogenation of 36. A solution of **36** (128 mg, 0.420 mmol) in ethyl acetate (30 mL) was hydrogenated over platinum oxide (10 mg) at atmospheric pressure for 15 min. Workup as before afforded 110 mg (86%) of **38**, colorless crystals, mp 150.5–151.5 °C (from ether); 1H NMR ($CDCl_3$) δ 4.55 (s, 2 H), 3.06 (br s, 2 H), 2.87 (s, 3 H), 1.90–1.33 (m, 11 H), 1.33–1.20 (m, 1 H), 0.83–0.60 (m, 2 H); ^{13}C NMR (ppm, $CDCl_3$) 158.95, 153.85, 75.01, 70.78, 52.72, 42.33, 32.82, 32.53, 26.26, 25.78, 25.10, 24.86; mass spectrum, m/e (M^+) calcd, 299.1634; obsd, 299.1643.

Anal. Calcd for $C_{17}H_{21}N_3O_2$: C, 68.20; H, 7.07. Found: C, 68.25; H, 7.07.

Catalytic Hydrogenation of 36/37 Mixture. A solution of the isomeric urazoles **36** and **37** (484 mg, 1.63 mmol) in ethyl acetate (30 mL) was hydrogenated in the predescribed manner. Solvent evaporation after filtration left a white solid which was analyzed by 1H and ^{13}C NMR and compared to authentic spectra. The ratio of **38** to **29** was 61.5:38.5.

Dimethyl syn- and anti-1',4',5',8'-Tetrahydrospiro[cyclopentane-1,9'-[1,4,5,8]dimethanonaphthalene]-6',7'-dicarboxylates (39 and 40). A solution of **4** (67.6 mg, 0.37 mmol) and dimethyl acetylenedicarboxylate (52.2 mg, 0.37 mmol) in $CDCl_3$ (2 mL) was prepared in an NMR tube.

Cycloaddition was observed to be complete within 15 h. The ratio of **39** to **40** was seen to be 78:22 (^{13}C NMR analysis). Following recording of this spectrum, the product mixture was directly hydrogenated.

For **39**: ^{13}C NMR (ppm, CDCl_3) 172.11, 166.38, 150.11, 140.40, 89.82, 68.75, 63.11, 51.80, 50.39, 34.03, 32.53, 25.54, 25.15.

For **40**: ^{13}C NMR (ppm, CDCl_3) 171.09, 166.14, 153.51, 143.56, 100.54, 78.79, 61.51, 51.80 (3 C), 34.57, 33.79, 25.54, 25.39.

Hydrogenation of 39 and 40. A 532 mg (1.63 mmol) sample of this mixture in ethyl acetate (20 mL) containing 20 mg of 5% Pd on charcoal was hydrogenated at atmospheric pressure for 30 min. Workup as before, followed by MPLC on silica gel (elution with 10% ethyl acetate in hexanes) afforded 210 mg of **31**, mp 75–76 °C, identical with the previously isolated sample, and 92 mg of **30** which likewise proved identical with the earlier sample.

Single-Crystal X-ray Diffraction Analysis of 5. A cubic crystal approximately 0.4 mm on an edge was selected for the diffraction experiment. Preliminary photographs showed only triclinic symmetry and accurate lattice constants, obtained from a least-squares fit of 15 diffractometer measured 2θ values, were $a = 6.234$ (1) Å, $b = 8.494$ (2) Å, $c = 13.313$ (3) Å, $\alpha = 82.89$ (2)°, $\beta = 87.57$ (2)°, and $\gamma = 100.36$ (2)°. Density considerations, $\rho_c = 1.29$ g/cm 3 for $Z = 2$, suggested that the unit cell contained two molecules of composition $\text{C}_{18}\text{H}_{18}\text{O}_2$ and we assumed that the space group was $P\bar{1}$. This assumption was confirmed by the subsequent analysis and refinement.

All unique diffraction maxima with $2\theta \leq 114^\circ$ were collected on an automated four-circle diffractometer using graphite monochromated Cu K α radiation (1.54178 Å) and variable-speed $1^\circ \omega$ scans. Of the 2026 reflections measured, 1978 (97%) were considered observed ($|F_o| \geq 3\sigma(F_o)$) after correction for Lorentz, polarization, and background effects. The angular dependence of the reflections was removed by using the Wilson plot and normalized structure factors were calculated.⁵¹ A phasing model was arrived at by using a multisolution sign determining procedure, and the E synthesis from this approach revealed all of the non-hydrogen atoms. Hydrogens were located on a difference synthesis following partial refinement. Block diagonal least-squares refinement with anisotropic non-hydrogen atoms and isotropic hydrogens has converged to a standard crystallographic residual of 0.044 for the observed reflections. Please consult the supplementary material for additional crystallographic details.

Single-Crystal X-ray Diffraction Analysis of 7. A suitable crystal with approximate dimensions 0.4 × 0.3 × 0.2 mm was selected for the single-crystal structure determination. Preliminary X-ray photographs revealed only triclinic symmetry and accurate lattice constants, determined by a least-squares fit of 15 diffractometer measured 2θ values, were $a = 8.707$ (2) Å, $b = 10.355$ (3) Å, $c = 10.949$ (2) Å, $\alpha = 114.00$ (2)°, $\beta = 97.90$ (2)°, and $\gamma = 106.40$ (2)°. Density considerations, $\rho_c = 1.31$ g/cm 3 for $Z = 2$, were assumed to indicate space group $P\bar{1}$ with one molecule of $\text{C}_{20}\text{H}_{22}\text{SO}_2$ forming the asymmetric unit. All unique diffraction maxima with $2\theta \leq 55^\circ$ were collected on an automated four-circle diffractometer using graphite monochromated Mo K α radiation (0.71069 Å) and a variable speed, $1^\circ \omega$ scan technique. Of the 3127 reflections surveyed, 2935 (94%) were considered observed ($|F_o| \leq 3\sigma(F_o)$) after correction for Lorentz, polarization, and background effects.

The structure was solved routinely by the heavy atom technique. The sharpened Patterson synthesis revealed the S position and the S-phased electron density synthesis revealed the non-hydrogen structure.⁵¹ Hydrogens were found on a difference synthesis following partial refinement. Full-matrix least-squares refinements with anisotropic non-hydrogen atoms and isotropic hydrogens have converged to a standard crystallographic residual of 0.054 for the observed reflections. Additional crystallographic details can be found in the supplementary material described at the end of this paper.

Single-Crystal X-ray Analysis of 25. Preliminary X-ray photographs revealed only triclinic symmetry and accurate lattice constants of $a = 8.426$ (2) Å, $b = 13.116$ (3) Å, $c = 14.641$ (3) Å, $\alpha = 78.70$ (2)°, $\beta = 76.48$ (2)°, and $\gamma = 90.18$ (2)° were determined from a least-squares fit of 15 moderate 2θ values. Approximate density considerations were consistent with one molecule of $\text{C}_{20}\text{H}_{22}\text{O}_2$ forming the asymmetric unit in the assumed space group $P\bar{1}$. All diffraction maxima with $2\theta \geq 114^\circ$ were collected on an automated four-circle diffractometer using graphite monochromated Cu K α radiation (1.54178 Å) and a variable-speed $1^\circ \omega$ scan. Of the 4380 reflections surveyed in this manner, 3962 (91%) were judged observed ($|F_o| \leq 3\sigma(F_o)$) after correction for Lorentz, polarization, and background effects.

A phasing model was achieved by using a multisolution sign-determining procedure,⁵² and an E synthesis of the most favorable set showed all of the non-hydrogen atoms. Most hydrogens were located on a difference synthesis following partial refinement but those on C(12) were included at calculated positions. Block-diagonal least-squares refinement with anisotropic non-hydrogen atoms and isotropic hydrogens have converged to a standard crystallographic residual of 0.067 for the observed reflections. Additional crystallographic details can be found in the supplementary material described at the end of this paper.

Single-Crystal X-ray Analysis of 29. Preliminary X-ray photographs of a suitable single crystal of **29** showed monoclinic symmetry. Accurate lattice parameters, determined from a least-squares fit of 15 moderate 2θ values, were $a = 7.382$ (2) Å, $b = 10.804$ (2) Å, $c = 15.035$ (3) Å, and $\beta = 91.91$ (2)°. The systematic absences were uniquely accommodated by space group $P2_1/c$, and density considerations suggested one molecule of $\text{C}_{17}\text{H}_{21}\text{N}_3\text{O}_2$ formed the asymmetric unit. All unique diffraction maxima with $2\theta \leq 55^\circ$ were collected with an automated four-circle diffractometer using graphite monochromated Mo K α (0.71069 Å) and a variable-speed $1^\circ \omega$ scan. Of the 4120 reflections surveyed in this manner, 2805 (68%) were judged observed ($|F_o| \geq 3\sigma(F_o)$) after correction for Lorentz, polarization, and background effects.

The structure was solved with a multisolution sign-determining procedure, and an E synthesis of the most favorable set showed 20 of the 22 non-hydrogen atoms. After partial refinement an F synthesis showed the entire molecule. A difference synthesis revealed most of the hydrogens, but those on C(20) were not clear and were input at calculated positions. Full-matrix least-squares refinement converged to a standard crystallographic residual of 0.065 for the observed reflections. Additional crystallographic details can be found in the supplementary material described at the end of this paper.

Photoelectron Spectroscopy. The He I PE spectra of **1** and **3** were recorded with a Perkin-Elmer Ltd. Model PS 18 instrument (Beaconsfield, England) and calibrated with Xe and Ar. A resolution of 20 meV at the $^2P_{3/2}$ Ar line was obtained.

Acknowledgment. Financial support for the research described herein was provided: (a) to LAP by the National Cancer Institute (Grant CA-12115); (b) to RG by the Fonds der Chemischen Industrie and BASF Aktiengesellschaft, Ludwigshafen; and (c) to JC by the National Cancer Institute (Grant CA-24487).

Registry No. 1, 81897-89-4; 2, 85222-06-6; 3, 81897-93-0; 4, 85222-07-7; 5, 85222-08-8; 6, 85280-07-5; 7, 85222-09-9; 8, 85280-08-6; 9, 85221-94-9; 13, 85222-10-2; 14, 85280-09-7; 15, 85222-11-3; 16, 85222-12-4; 17, 85222-13-5; 18, 85222-14-6; 19, 85222-15-7; 20, 85222-16-8; 21, 85222-17-9; 22, 85222-18-0; 23, 85222-19-1; 24, 85222-20-4; 25, 85222-21-5; 26, 85234-91-9; 27, 85222-22-6; 28, 85222-23-7; 29, 85222-24-8; 30, 85222-25-9; 31, 85280-10-0; 32, 85222-26-0; 33, 85222-27-1; 34, 85280-11-1; 35, 85280-12-2; 36, 85222-28-2; 37, 85280-13-3; 38, 85280-14-4; 39, 85222-29-3; 40, 85280-15-5; benzoquinone, 106-51-4; *N*-phenylmaleimide, 941-69-5; dimethyl acetylenedicarboxylate, 762-42-5; phenyl vinyl sulfone, 5535-48-8; *N*-methyltriazolinedione, 13274-43-6; maleic anhydride, 108-31-6.

Supplementary Material Available: Tables of fractional coordinates, thermal parameters, bond distances, bond angles and observed and calculated structure factors for **5**, **7**, **25**, and **29** (72 pages). Ordering information is given on any current masthead page.

(52) All crystallographic calculations were done on a PRIME 400 computer operated by the Materials Science Center and the Department of Chemistry, Cornell University. The principal programs used were REDUCE and UNIQUE, data reduction programs, Leonowicz, M. E., Cornell University, 1978; BLS78A, anisotropic block-diagonal least-squares refinement, Hirotsu, K. and Arnold, E., Cornell University, 1980; SRAY76, the X-ray System of Crystallographic Programs, edited by Stewart, J. M., University of Maryland, Technical Report TR-445, March 1976; ORTEP, crystallographic illustration program, Johnson, C. K.; Oak Ridge, ORNL-3794; BOND, molecular metrics program, Hirotsu, K., Cornell University, 1978; MULTAN-78, "A System of Computer Programs for the Automatic Solution of Crystal Structures from X-ray Diffraction Data", University of York, England. Principal author P. Main. For literature description of MULTAN, see: Germain, G.; Main, P.; Woolfson, M. M. *Acta Crystallogr., Sect. B* 1970, B26, 274–285. Woolfson, M. M. *Acta Crystallogr., Sect. A* 1977, A33, 219–225.